FE ISOTOPE NUCLEOSYNTHESIS: CONSTRAINTS FROM FE ISOTOPIC ANALYSES OF PRESOLAR SILICATE GRAINS FROM ACFER 094.

W. J. Ong and C. Floss. Laboratory for Space Sciences and Physics Department, Washington University, St. Louis, MO, USA (Contact email: floss@wustl.edu)

Introduction: Presolar grains provide information about fundamental astrophysical processes, such as stellar nucleosynthesis and galactic chemical evolution. Iron is of particular interest because of its importance in s-process nucleosynthesis. However, the data (largely from presolar SiC grains [1, 2]) show some inconsistencies with the compositions predicted from current stellar models, both for mainstream grains of AGB origin and for X grains from supernovae.

Presolar silicate grains are good candidates for Fe isotopic measurements because many have high Fe contents [3-6], but the analyses are technically challenging due to their small sizes and the fact that they are typically identified in meteorite thin sections or densely packed grain size separates. Here we report on our ongoing efforts [e.g., 7] to determine the Fe isotopic compositions of presolar silicate grains.

Experimental: Isotopically anomalous grains were initially identified through NanoSIMS C and O raster ion imaging [e.g., 3] of a 0.1 – 0.5 µm Acfer 094 grain size separate. Elemental compositions were determined using Auger spectroscopy in order to identify suitable grains for the Fe isotopic analyses.

In order to mitigate some of the problems associated with carrying out Fe isotopic measurements using a O^- primary ion beam (e.g., substantial signal contamination, difficulty in locating the grains for analysis), we are using the Cs^+ primary ion beam of the NanoSIMS and measuring the Fe isotopes as oxides [7]. The measurements are done in grain mode, using two magnetic fields and the following masses: 16 (^{16}O), 68 (^{52}CrO), 70 (^{54}FeO, ^{54}CrO), 73 (^{57}FeO), and 78 (^{62}NiO) in detectors 1–5, followed by 72 (^{56}FeO) and 74 (^{58}FeO, ^{58}NiO) in detectors 2–3. Following acquisition of a 10 x 10 µm^2 image of the area of interest, the beam is rastered over individual grains selected from this image. The measurements were made at a mass resolution high enough to largely separate $^{56}Fe^{16}OH^-$ from $^{57}Fe^{16}O^-$. Measurements on an FeNi standard show a contribution from $^{56}Fe^{16}OH^-$ to the $^{57}Fe^{16}O^-$ peak of ~ 1% and a reproducibility of ~20‰ for both $^{57}Fe/^{56}Fe$ and $^{54}Fe/^{56}Fe$ [7]. The contribution from the ^{56}FeO hydride peak is greater in the silicate analyses (~10%), but the reproducibility for both ratios is also ~20–30‰ for isotopically normal matrix grains in the vicinity of each presolar grain measured, indicating a relatively stable hydride contribution in the different grains.

Corrections were made for ^{54}Cr on ^{54}Fe, based on the measured $^{52}Cr^{16}O^-$, assuming solar Cr isotopic compositions, and were ≤ ~10‰ for all of the grains measured. No data are reported for $^{58}Fe/^{56}Fe$, as the $^{58}Fe^{16}O^-$ signal is dominated by contributions from $^{58}Ni^{16}O^-$ and no meaningful corrections could be made. The data were normalized to the average compositions of the normal matrix grains measured in the vicinity of each presolar grain.

Results: Figure 1 shows the O isotopic compositions of the 13 grains analyzed for Fe isotopes. Most are Group 1 grains, with enrichments in ^{17}O and close-to-solar $^{18}O/^{16}O$ ratios. Two grains show enrichments in both ^{17}O and ^{18}O and can be considered Group 4 grains. Fe contents of the grains range from 10–43 at.%. Two grains (12-5 and 16-12) are Fe-oxides, as is grain 34C-10 [8]. The remaining grains are silicates.

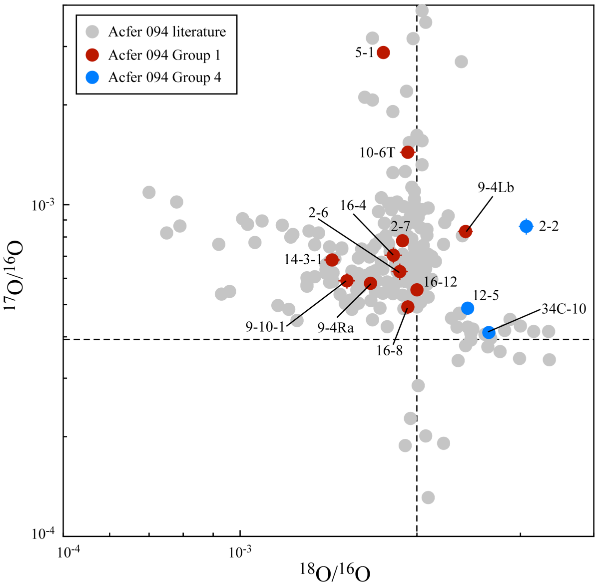

Figure 1. Oxygen isotopic compositions of presolar grains from Acfer 094. Also shown is Acfer 094 FeO grain 34C-10 [8]. Literature data are from the Presolar Grain Database [9].

The Fe isotopic compositions of the grains are shown in Fig. 2. Six grains have normal $^{54}Fe/^{56}Fe$ and $^{57}Fe/^{56}Fe$ ratios. Five additional grains have normal $^{54}Fe/^{56}Fe$, but show depletions in ^{57}Fe; the depletions are relatively modest in four of these, with $^{57}Fe/^{56}Fe$ ratios that are within 2–3σ of the solar value, but grain 2-7 shows a much larger depletion ($\delta^{57}Fe = -210 \pm 35$ ‰). Grain 34C-10 is depleted in both ^{54}Fe and ^{57}Fe [8]. Finally, one grain, 14-3-1, is enriched in ^{57}Fe ($\delta^{57}Fe = 145 \pm 35$ ‰) and another, 16-8, is enriched in both ^{54}Fe and ^{57}Fe ($\delta^{54}Fe = 70 \pm 25$ ‰; $\delta^{57}Fe = 80 \pm 30$ ‰).

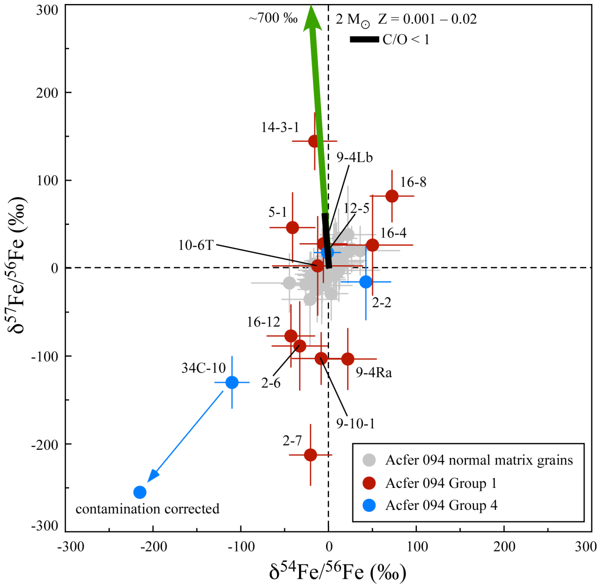

Figure 2. Fe isotopic compositions of presolar grains from Acfer 094. Also shown are AGB model predictions from FRUITY [10]. Errors are 1σ.

Discussion: Group 1 grains come from low-mass AGB stars of close-to-solar metallicity. Neutron capture in the He intershell during the thermally pulsing phase [e.g., 11] consumes ^{54}Fe and ^{56}Fe and produces ^{57}Fe and ^{58}Fe. Thus, ^{54}Fe/^{56}Fe ratios are not expected to change substantially from the initial values of the parent stars, whereas the ^{57}Fe/^{56}Fe and ^{58}Fe/^{56}Fe ratios will be elevated. Figure 2 shows model predictions for 2 M$_\odot$ AGB stars with metallicities from 0.001 – 0.02 [10]; shown are the isotopic compositions expected in the envelope during the third dredge-up. The models predict enrichments in ^{57}Fe of up to about 700 ‰; however, in the early dredge-up episodes where the C/O ratios are <1 and O-rich grains are more likely to form, the enhancements in ^{57}Fe are less, on the order of about 50 ‰.

The normal ^{54}Fe/^{56}Fe ratios in most of our Group 1 grains are consistent with the model predictions, as are the solar ^{57}Fe/^{56}Fe values in several grains, and the ^{57}Fe enrichments observed in grains 14-3-1 and 16-8. Grain 16-8 is also enriched in ^{54}Fe, which is not expected. Under-correction of the ^{54}Cr contribution is possible, but not likely, since the corrections were very small for all grains. Another possibility is galactic chemical evolution, which is expected to produce large changes in ^{54}Fe/^{56}Fe ratios [e.g., 1]. More difficult to understand, however, are the depletions in ^{57}Fe that we observe in several grains, particularly in grain 2-7. Similar ^{57}Fe deficits have also been seen in some mainstream SiC grains [1]. Such deficits are not predicted by current AGB models.

Our Group 4 grains, 2-2 and 12-5, have normal ^{54}Fe/^{56}Fe and ^{57}Fe/^{56}Fe ratios. Their O isotopic compositions suggest formation in the H envelope with some contribution from the He/C zone, which is enriched in ^{18}O. Figure 3 shows the distribution of Fe isotopes in the interior zones of a 15 M$_\odot$ supernova model [12]. Normal Fe isotopic ratios in the He/N zone and H envelope and close-to-normal ratios in the He/C zone are consistent with the Fe isotopic compositions of these two grains.

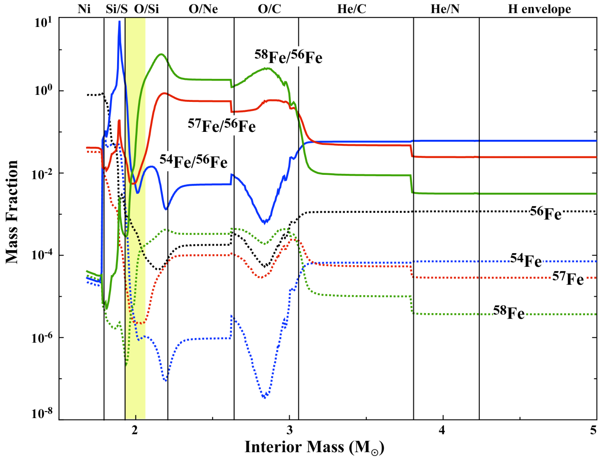

Figure 3. Fe isotopic compositions in the interior zones of a 15 M$_\odot$ supernova model [12].

However, FeO grain 34C-10, a Group 4 grain enriched in ^{18}O, shows significant depletions in both of these isotopes [8], and these are more difficult to understand. The only region with depletions in both ^{54}Fe and ^{57}Fe is a small pocket in the O/Si zone. Mixing with this pocket can reproduce the Fe isotopic composition of grain 34C-10, but leads to depleted ^{18}O/^{16}O and ^{17}O/^{16}O compositions, because this zone is strongly enriched in ^{16}O. Both the O and Fe isotopic compositions could be explained if the grain condensed initially in the O/Si zone as Fe metal and was later oxidized to FeO. However, it seems unlikely that reduced Fe metal would condense in such an O-rich zone. Similar problems exist with some SiC X grains, which also have deficits in ^{57}Fe [1] and which are also not likely to condense in the O-rich O/Si zone where ^{57}Fe depletions are observed.

References: [1] Marhas et al. (2008) *ApJ* 689, 622. [2] Trappitsch et al. (2012) *LPS XLIII*, #2497. [3] Floss and Stadermann (2009) *GCA* 73, 2415. [4] Vollmer et al. (2009) *GCA* 73, 7127. [5] Bose et al. (2010) *ApJ* 714, 1624. [6] Nguyen et al. (2010) *ApJ* 719, 166. [7] Ong et al. (2012) *LPS XLIII*, #1225. [8] Floss et al. (2008) *ApJ* 672, 1266. [9] Hynes and Gyngard (2009) *LPS XL*, #1198. [10] Cristallo et al. (2011) *ApJS* 197, 17. [11] Busso et al. (1999) *ARAA* 37, 239. [12] Rauscher et al. (2002) *ApJ* 576, 323.

This work is supported by NASA grant NNX10AH07G (C.F.).